2012-03-06

Association of common genetic variants in GPCPD1 with scaling of visual cortical surface area in humans

Trygve E. Bakken
University of California at San Diego

Et al.

Association of common genetic variants in GPCPD1 with scaling of visual cortical surface area in humans

Trygve E. Bakken[a,b], J. Cooper Roddey[c], Srdjan Djurovic[d,e], Natacha Akshoomoff[f,g], David G. Amaral[h], Cinnamon S. Bloss[b], B. J. Casey[i], Linda Chang[j], Thomas M. Ernst[j], Jeffrey R. Gruen[k], Terry L. Jernigan[f,g,l,m], Walter E. Kaufmann[n], Tal Kenet[o], David N. Kennedy[p], Joshua M. Kuperman[m], Sarah S. Murray[b], Elizabeth R. Sowell[q,r], Lars M. Rimol[d], Morten Mattingsdal[d,s], Ingrid Melle[d,s], Ingrid Agartz[d,t], Ole A. Andreassen[d,s], Nicholas J. Schork[b,u,1], Anders M. Dale[c,m,1], for the Alzheimer's Disease Neuroimaging Initiative[2], and Pediatric Imaging, Neurocognition, and Genetics Study[2]

[a]Medical Scientist Training Program, University of California at San Diego, La Jolla, CA 92093; [b]Scripps Genomic Medicine and Scripps Translational Science Institute, The Scripps Research Institute, La Jolla, CA 92037; [c]Department of Neurosciences, University of California at San Diego, La Jolla, CA 92093; [d]Institute of Clinical Medicine, University of Oslo, 0450 Oslo, Norway; [e]Department of Medical Genetics, Oslo University Hospital, 0424 Oslo, Norway; [f]Center for Human Development, University of California at San Diego, La Jolla, CA 92093; [g]Department of Psychiatry, University of California at San Diego, La Jolla, CA 92093; [h]Department of Psychiatry and Behavioral Sciences, University of California at Davis, Sacramento, CA 95817; [i]Sackler Institute for Developmental Psychobiology, Weill Cornell Medical College, New York, NY 10065; [j]Department of Medicine, University of Hawaii and Queen's Medical Center, Honolulu, HI 96813; [k]Departments of Pediatrics and Genetics, Yale University School of Medicine, New Haven, CT 06520; [l]Department of Cognitive Science, University of California at San Diego, La Jolla, CA 92093; [m]Department of Radiology, University of California at San Diego, La Jolla, CA 92093; [n]Kennedy Krieger Institute, Johns Hopkins University School of Medicine, Baltimore, MD 21205; [o]Department of Neurology and Athinoula A. Martinos Center for Biomedical Imaging, Massachusetts General Hospital, Charlestown, MA 02129; [p]Department of Psychiatry, University of Massachusetts Medical School, Worcester, MA 01605; [q]Department of Pediatrics, University of Southern California, Los Angeles, CA 90027; [r]Department of Pediatrics, Children's Hospital Los Angeles, Los Angeles, CA 90027; [s]Division of Mental Health and Addiction, Oslo University Hospital, 0424 Oslo, Norway; [t]Department of Research and Development, Diakonhjemmet Hospital, 0319 Oslo, Norway; and [u]Department of Molecular and Experimental Medicine, The Scripps Research Institute, La Jolla, CA 92037

Edited* by Charles F. Stevens, The Salk Institute for Biological Studies, La Jolla, CA, and approved January 17, 2012 (received for review April 12, 2011)

Visual cortical surface area varies two- to threefold between human individuals, is highly heritable, and has been correlated with visual acuity and visual perception. However, it is still largely unknown what specific genetic and environmental factors contribute to normal variation in the area of visual cortex. To identify SNPs associated with the proportional surface area of visual cortex, we performed a genome-wide association study followed by replication in two independent cohorts. We identified one SNP (rs6116869) that replicated in both cohorts and had genome-wide significant association ($P_{combined} = 3.2 \times 10^{-8}$). Furthermore, a metaanalysis of imputed SNPs in this genomic region identified a more significantly associated SNP (rs238295; $P = 6.5 \times 10^{-9}$) that was in strong linkage disequilibrium with rs6116869. These SNPs are located within 4 kb of the 5′ UTR of *GPCPD1*, glycerophosphocholine phosphodiesterase GDE1 homolog (*Saccharomyces cerevisiae*), which in humans, is more highly expressed in occipital cortex compared with the remainder of cortex than 99.9% of genes genome-wide. Based on these findings, we conclude that this common genetic variation contributes to the proportional area of human visual cortex. We suggest that identifying genes that contribute to normal cortical architecture provides a first step to understanding genetic mechanisms that underlie visual perception.

allometry | brain morphometry | imaging genetics | V1

Primates, including humans, rely on vision to navigate their environment, find food, and avoid predators. Visual performance varies between primate species partly because of genetic variation, and better vision may have provided an evolutionary fitness advantage. For example, allelic diversity of visual pigments in the eye evolved convergently in apes, Old World monkeys, and howler monkeys (1) and enabled red–green color discrimination, enhancing these primates' ability to identify sources of food (2).

Visual performance also varies within primate species, such as between human individuals (3), and this performance may be correlated with the number of neurons available to process visual information. Indeed, two studies of healthy human subjects found that increased surface area of primary visual cortex (V1) and thus, more neurons in V1 (4) were associated with increased Vernier acuity (5) and decreased susceptibility to two optical illusions (6). It is striking that visual cortical surface area is associated with optical illusion strength, because this result implies that the number of neurons in V1 can explain human variation in the conscious perception of seemingly physically identical stimuli.

Individuals have highly variable portions of their brains devoted to visual processing, because the surface areas of visual cortical regions (e.g., V1, V2, and V3 in the occipital lobe) are correlated and vary two- to threefold in humans (7, 8). This variation is significantly greater than variation in total cortical area, and therefore, both the absolute area and proportion of the cortical sheet allocated to processing vision varies between individuals. Moreover, a recent human twin study showed strong genetic correlations between the area of V1 and the remainder of occipital cortex but not other cortical lobes (9), suggesting that occipital visual areas share common genetic influences. However, it is still largely unknown what specific genetic and environmental factors contribute to normal variation in the absolute and proportional size of occipital cortex. To address this question, we performed a genome-wide association study (GWAS) to identify SNPs associated with the proportional surface area of occipital cortex in two independent human cohorts.

Human twin studies have shown a significant genetic component to cortical volume (10–12) and surface area (>80% heritable) (13–16), and the occipital proportion of cortex is also quite

Author contributions: S.D., N.A., D.G.A., C.S.B., B.J.C., L.C., T.M.E., J.R.G., T.L.J., W.E.K., T.K., D.N.K., J.M.K., S.S.M., E.R.S., I.M., I.A., O.A.A., and A.M.D. designed research; T.E.B., J.C.R., S.D., L.M.R., M.M., N.J.S., and A.M.D. performed research; J.M.K., A.D.N.I. and P.I.N.G. contributed new reagents/analytic tools; T.E.B., J.M.K., and A.M.D. analyzed data; T.E.B., O.A.A., N.J.S., and A.M.D. wrote the paper; and A.D.N.I. and P.I.N.G. provided MRI and genotype data.

Conflict of interest statement: I.M. has received a speaker's honorarium from Janssen and AstraZeneca. I.A. has served as an unpaid consultant for Eli Lilly. O.A.A. has received a speaker's honorarium from AstraZeneca, Janssen, Bristol-Myers Squibb, and GlaxoSmithKline. A.M.D. is a founder and holds equity in CorTechs Labs and also serves on its Scientific Advisory Board. Eli Lilly supported parts of the genotyping costs for the Thematic Organized Psychoses Study sample. The terms of this arrangement have been reviewed and approved by the University of California at San Diego in accordance with its conflict of interest policies. All other authors report no conflict of interest.

*This Direct Submission article had a prearranged editor.

[1]To whom correspondence may be addressed. E-mail: nschork@scripps.edu or amdale@ucsd.edu.

[2]A complete list of the Alzheimer's Disease Neuroimaging Initiative and Pediatric Imaging, Neurocognition, and Genetics Study authors can be found in the *SI Appendix*.

This article contains supporting information online at www.pnas.org/lookup/suppl/doi:10.1073/pnas.1105829109/-/DCSupplemental.

heritable (25–50%) (11, 13). These studies reveal that genes have both global and regional effects on cortical surface area, which also seems to be true in mice. For example, the work by Airey et al. (17) reported that two strains of inbred mice with different genetic backgrounds have different proportions of cortex allocated to primary visual and somatosensory cortex, and these strains can be reliably discriminated based on these regional as well as global measures of cortical surface area.

Furthermore, specific homeobox transcription factors (e.g., *EMX2* and *PAX6*) have been identified that are expressed in gradients across the surface of the mouse brain during neural development and control the anterior–posterior distribution of cortical areas (18, 19). Cortex-specific overexpression of *EMX2* in mice resulted in an expansion of occipital areas and a corresponding reduction in sensory and motor areas that led to dysfunctional tactile and motor behaviors (20). Similarly, *EMX2* and *PAX6* may be expressed in gradients during neural development in human subjects (21), and individuals with protein coding mutations in *PAX6* (22, 23) exhibit cortical malformations. In addition, *EMX2* mutations have been associated with schizencephaly, a rare cortical developmental disorder (24, 25), although these mutations likely explain a small fraction of this disease burden (26, 27). Finally, mutations in the laminin gene *LAMC3* have been associated with cortical malformations solely within the occipital lobe (28), providing additional evidence for genetic control over regional cortical development.

Genetic variants may also mediate more subtle variation in human cortical structure. For example, two candidate gene studies recently identified SNPs in microcephaly genes (29) and *MECP2* (30) that explained a small but statistically significant amount of variation in total cortical surface area between human individuals and were replicated in independent study populations.

In this study, we extend the analysis of the datasets used in those studies in two ways. First, we performed an unbiased GWAS rather than selecting candidate genes to identify genetic loci that contribute to normal variation in human cortical structure. Second, we analyzed the scaling of occipital cortical surface area with total cortical area because of the evidence from mice and human twin studies that this scaling relationship may be under independent genetic control from overall brain size.

Results

In a sample of 421 human subjects with Norwegian ancestry from the Thematic Organized Psychoses (TOP) study, we found that occipital cortical surface area is highly correlated with total cortical area ($r = 0.85$, $P = 3.1 \times 10^{-118}$). The occipital cortex occupied, on average, 12.1% of total cortical surface area regardless of brain size, and the occipital fraction of cortex ranged from 11.1% to 14.8% in all subjects. We hypothesized that this variation was partly because of genetic differences between subjects. Therefore, we tested SNPs genome-wide for their effect on the scaling relationship between occipital and total cortical surface area. Specifically, we tested each SNP in a GWAS for the strength of the interaction between the SNP minor allele account and total cortical surface area in predicting occipital cortical surface area, while controlling for sex, age, and diagnosis. This interaction effect would reflect the degree to which the SNP accentuated the influence of overall cortical surface area on occipital cortical surface area (i.e., modified the scaling relationship between total and occipital cortical surface area).

One SNP (rs6116869; minor allele frequency = 0.36) showed strong interaction association ($P = 7.75 \times 10^{-8}$, $\beta = 0.0285$, SE = 0.0052, $n = 413$) with occipital cortical surface area, although this SNP did not quite reach genome-wide significance ($P < 5 \times 10^{-8}$). A quantile–quantile plot of $-\log_{10}$ (P values) from the GWAS revealed moderate genomic inflation ($\lambda_{GC} = 1.25$), and this inflation suggested that the original SNP P value may have been artificially low. Thus, we sought a more accurate estimate of the P value in two ways: (*i*) accounting for genetic relatedness between subjects and (*ii*) permutation testing. In addition, we tested the SNP for association in two independent replication cohorts and interaction association with surface area across the whole cortex. Finally, we investigated the cortical expression pattern of *GPCPD1*, a nearby gene, in two human brains.

First, despite the fact that subjects were unrelated and self-reported Norwegian ancestry, we hypothesized that subtle population structure or cryptic relatedness could have compromised the statistical independence of subjects. A lack of independence would have decreased SNP variance estimates and associated P values, resulting in genomic inflation. We approximated population structure in our study by using principle components analysis (PCA) to estimate major axes of variation of genome-wide allele frequencies. We repeated the GWAS and controlled for sex, age, and diagnosis as well as population structure along the first four axes from the PCA, which has been shown to help correct for population stratification (31). We found that genomic inflation was slightly reduced ($\lambda_{GC} = 1.23$), and rs6116969 association was now genome-wide significant ($P = 4.95 \times 10^{-8}$, $\beta = 0.0289$, SE = 0.0052). We performed genomic control, and rs6116869 still showed markedly stronger association ($P_{GC} = 8.79 \times 10^{-7}$, $\beta = 0.0289$, $SE_{GC} = 0.0058$) than other SNPs (Fig. 1 and Figs. S1 and S2).

Next, we used permutation tests to estimate the significance of rs6116869 association, and the permuted P value ($P_{perm} = 6 \times 10^{-7}$) supported the genomic control P value, suggesting that genomic control had effectively corrected for inflation. Thus, for the remainder of the analysis, we report the conservative genomic control SEs and P values.

Given the significant interaction effect between rs6116869 and total cortical area, we expected that the slope of the linear regression that related occipital to total cortical surface area would vary based on rs6116869 genotype. Indeed, we found that each copy of the SNP minor allele increased the slope by 28% (Fig. 2*A*). On average, the occipital cortex of subjects heterozygous for rs6116869 (GT genotype; $n = 184$) occupied 12.7% of total cortical surface area, and this occipital proportion was independent of total cortical area (Fig. 2*B*). In contrast, subjects homozygous for the major allele (GG; $n = 171$) had an occipital proportion that decreased from 13.2% to 12.6%, on average, over the range of total cortical areas observed in our study. Inversely, subjects homozygous for the minor allele (TT; $n = 58$)

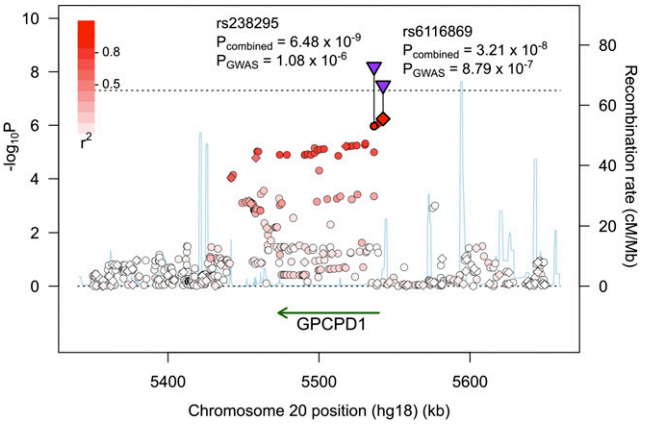

Fig. 1. Genomic region showing the strongest SNP association with occipital cortical area scaling. Genotyped (◇) and imputed (○) SNPs are colored based on linkage disequilibrium (r^2) with rs6116869. Combined P values for rs6116869 and rs238295 (▽) are genome-wide significant ($P < 5 \times 10^{-8}$; dotted line) based on a metaanalysis of the GWAS and two replication studies. rs238288 is not labeled and is located in between these two SNPs. P values are corrected for genomic inflation.

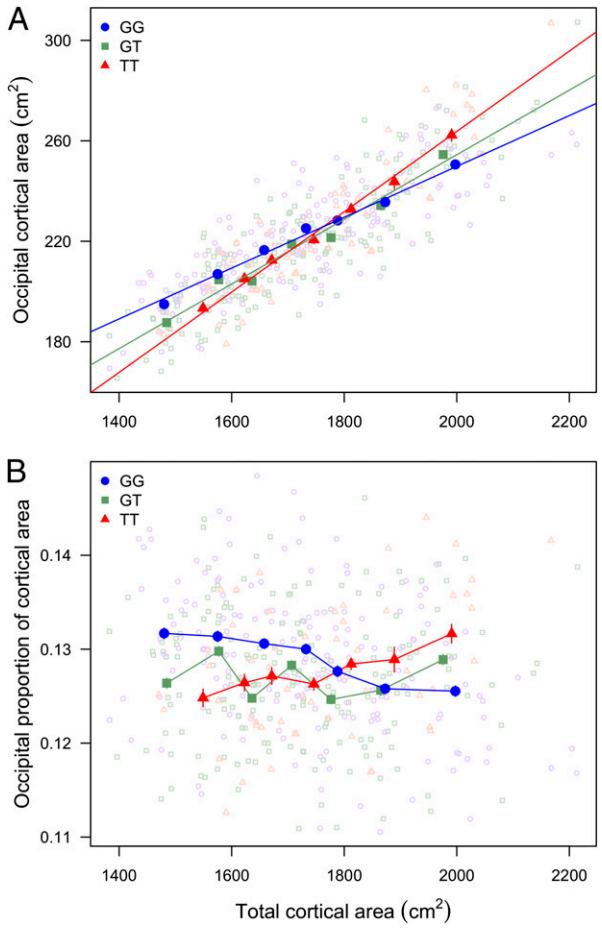

Fig. 2. Occipital cortical area scaling varies by rs6116869 genotype. (*A*) The slope of occipital cortical area scaling with total cortical area increases with the number of minor alleles. For each genotype, subjects are grouped into seven bins with an equal number of subjects in each bin (24, 26, and 8 subjects per bin for genotypes GG, GT, and TT, respectively). Binned averages ± SEM (dark) and regression lines fit to individual (light) measures are plotted. (*B*) Occipital proportion of cortex varies based on total cortical area and genotype. Subjects are binned as in *A*, and occipital proportions (occipital area divided by total cortical area) are plotted for individuals (light). Binned averages ± SEM (dark) are indicated.

had an occipital proportion that increased from 12.5% to 13.2% over this same range. These 0.6% differences in the occipital proportion of cortex based on rs6116869 genotype represented a difference in absolute occipital cortical area of ~11 cm^2, equal to almost one-half the area of V1 (6). Therefore, for example, in the subset of subjects with relatively large total cortical surface area (~2,000 cm^2), subjects with the GG genotype had an occipital cortical area of 251 cm^2, whereas subjects with the TT genotype had an occipital cortical area of 262 cm^2.

We sought to replicate the rs6116869 association with occipital cortical area in two independent cohorts. First, we used 482 subjects—healthy controls or diagnosed with mild cognitive impairment (MCI)—from the Alzheimer's Disease Neuroimaging Initiative (ADNI) dataset who clustered with European reference populations based on genome-wide genotype data. rs238288 was the closest proxy for rs6116869 that was genotyped in the ADNI sample, and this SNP was highly correlated ($r^2 = 0.96$ in HapMap CEU population with northwestern European ancestry) with and 2.5 kb upstream from rs6116869. We tested rs238288 for a significant interaction with total cortical surface area in predicting occipital cortical surface area with the identical test used in the GWAS (i.e., controlling for sex, age, diagnosis, and population structure). We found modest genomic inflation ($\lambda_{GC} = 1.19$) (Fig. S3) in the ADNI study that was comparable with the inflation observed in the TOP study. rs238288 was significantly associated before (one-tailed $P = 0.0083$, $\beta = 0.0123$, SE = 0.0051, $n = 477$) and after ($P_{GC} = 0.015$) genomic control.

For our second replication cohort, we selected 278 subjects (aged 6–21 y old) from the Pediatric Imaging, Neurocognition, and Genetics (PING) study who clustered with European reference populations based on genome-wide genotype data. We excluded PING subjects younger than 6 y, because brain volume increases more than fourfold after birth and then, is mostly stable from age 6 y to adulthood (32). Likewise, cortical surface area decreases less than 10% during adolescence between the ages of 6 and 22 y (33), and therefore, we expected that the effect of genetic variation on the scaling of occipital cortical area would have occurred earlier in development and would be apparent in this younger replication cohort. Indeed, we found that rs238288 (the closest proxy for rs6116869) provided a second replication of the GWAS result (one-tailed $P = 0.018$, $\beta = 0.0208$, SE = 0.0098, $n = 278$). No genomic inflation was observed in this dataset ($\lambda_{GC} = 1.00$). The combined P value for rs6116869 from the GWAS and two replication studies was genome-wide significant ($P_{combined} = 3.21 \times 10^{-8}$) based on an inverse variance-weighted z score (34).

To refine the association of this genetic locus with occipital cortical area scaling, we imputed SNPs for the TOP, ADNI, and PING samples in a 300-kb window around rs6116869 and performed a metaanalysis of these SNPs. We combined the genomic controlled P values for the imputed SNPs from the three studies (Fig. 1), and we identified the SNP (rs238295) that was most significantly associated ($P_{combined} = 6.48 \times 10^{-9}$). rs238295 was highly correlated with and proximal to both rs6116869 ($r^2 = 0.88$, 6 kb upstream) and rs238288 ($r^2 = 0.84$, 3.5 kb upstream).

Given the finite extent of the cortex, we expected that a relative increase in occipital cortical surface area would be associated with a compensatory decrease in surface area in other cortical regions. Therefore, we performed a region of interest analysis in the TOP, ADNI, and PING samples and tested rs238295 for association with 66 regions defined by cortical folding patterns. For each cortical region, we calculated the genomic inflation adjusted P value for the interaction between rs238295 and total cortical surface area, and we combined these P values from the three studies (Table S1). As expected, we found that rs238295 was strongly associated with the surface area of occipital cortical regions, including the bilateral pericalcarine area that is highly correlated with the V1 area (7) as well as lingual and lateral occipital areas. Intriguingly, rs238295 was also significantly associated with left superior and lateral temporal cortical areas in all three studies but in the opposite direction relative to the association with occipital cortical area. Thus, individuals homozygous at rs238295 with a relatively large occipital cortex had a relatively small left temporal cortex and vice versa.

To better visualize the SNP association with different cortical regions in the TOP cohort, we tested the interaction association of rs6116869 with total cortical area at each location across the cortical surface. A cortical map of $-\log_{10}$ (P values) broadly supported the region of interest analysis and also highlighted significant SNP associations with bilateral superior frontal cortical regions in the TOP study (Fig. 3).

The genotyped SNP that was most significantly associated with the occipital cortical area in the TOP sample (rs6116869) is located ~3 kb upstream of the protein coding gene *GPCPD1*, glycerophosphocholine phosphodiesterase GDE1 homolog (*Saccharomyces cerevisiae*), and the most significant imputed SNP in the combined analysis of both TOP and ADNI samples (rs238295) is located 6 kb downstream in the first intron of *GPCPD1*. These SNPs are at the end of a 100-kb linkage disequilibrium block

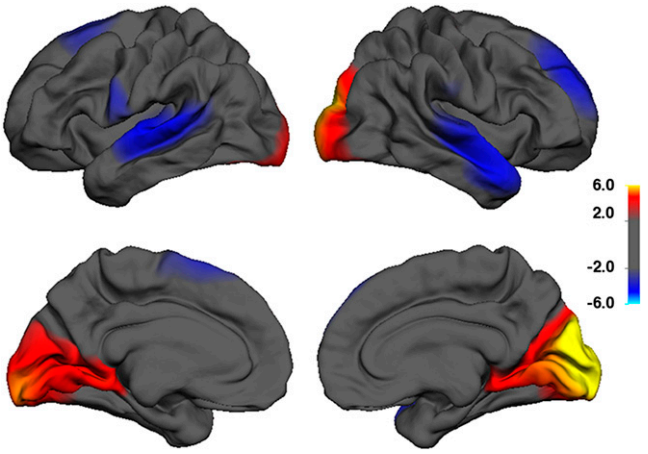

Fig. 3. *P* value map ($-\log_{10}$ *P* value) of rs6116869 association with cortical area scaling at each vertex across the surface of the brain, while controlling for age, sex, and diagnosis. Hot colors indicate increased scaling slope with the number of SNP minor alleles among subjects in the TOP study, and cool colors indicate decreased scaling slope with the number of SNP minor alleles among subjects in the TOP study.

that spans the full length of the gene, and this block includes a DNA sequence just upstream of the promoter to 30 kb distal to the 3′ UTR.

We explored the cortical expression pattern of *GPCPD1* in two adult brains using the Allen Human Brain Atlas (35), and we found that this gene had 1.5-fold greater expression specifically in occipital cortex compared with other cortical regions (Fig. S4). This relatively higher occipital expression was supported by two independent probes used to assess *GPCPD1* expression in both brains and more significant ($P = 2.1 \times 10^{-19}$) than 99.9% of genes (all but 11 genes) genome-wide (*SI Materials and Methods*).

Discussion

We performed a GWAS of occipital cortical area scaling with total cortical surface area in human individuals, and we identified one SNP (rs6116869) that showed strong association ($P = 8.8 \times 10^{-7}$) and replicated in two independent cohorts with a combined *P* value that was genome-wide significant ($P_{combined} = 3.2 \times 10^{-8}$). A metaanalysis of nearby SNPs identified rs238295, in strong linkage disequilibrium with rs6116869, as the most significantly associated SNP ($P_{combined} = 6.5 \times 10^{-9}$). Furthermore, rs238295 was associated with the scaling of left temporal cortical area in opposition to the scaling of occipital cortical area. These SNPs are located near the 5′ UTR of *GPCPD1*, a gene that is more highly expressed in the occipital cortex compared with other cortical regions in the adult human brain than virtually any other gene.

In humans, components of the visual system—retina, optic nerve, and visual thalamus and cortex (V1, V2, and V3)—scale in size together (7, 8). Moreover, mammalian brain size explains more than 95% of the variation in size of individual brain components, including neocortex, presumably because of evolutionarily conserved constraints on neural development (36). However, there is also evidence for mosaic brain evolution, when sets of functionally or anatomically linked brain structures have evolved independently of brain size (37). For example, although visual thalamus and V1 are highly correlated in size in primates, including humans, these visual structures are significantly smaller than would be expected for a nonhuman primate with a brain of human size (38). The mosaic evolution of primary visual cortical surface area among primates suggests that this region was under independent genetic control from the remainder of cortex on the evolutionary lineage leading to modern humans. Genetic variation between primate species that explains differences in the relative sizes of visual cortex may contribute to the two- to threefold variation in surface area of visual cortical regions observed between human individuals.

We found that the proportional area of occipital cortex varied by 33% between individuals (range = 0.11–0.15), and this phenotype showed the same pattern of association with rs238295 as the absolute occipital cortical area. Likewise, the work by Schwarzkopf et al. (6) found that illusion strength was significantly correlated with both the absolute and proportional sizes of primary visual cortex. If a larger fraction of the cortex is allocated to visual processing, then less cortical area and likely, fewer neurons (4, 39) are available to process information in other cortical regions. We found that left superior and lateral temporal cortical surface area was significantly decreased in individuals with relatively large visual cortical area. If this slight reduction in cortical area is associated with decreased information processing capacity, then one could potentially measure subtle changes in auditory processing, including language, which is associated with the left superior temporal gyrus (40). However, more studies are needed to confirm the microstructural basis for MRI measurements of cortical surface area in healthy adults. In addition, studies must distinguish whether absolute or relative cortical surface area is under more direct genetic control and which measure has more functional relevance.

We observed moderate genomic inflation in both the TOP and ADNI studies, although there were no clear outlier measurements of occipital cortical area in either cohort, and residuals from the linear models did not deviate significantly from normality in the TOP ($P = 0.63$) or ADNI ($P = 0.44$) studies using a sensitive Shapiro–Wilk test. Although we could attribute only a small part of this inflation to population stratification, subtle population structure or cryptic relatedness may have contributed to the genomic inflation. In any case, the consistency between the *P* values obtained with permutation testing and genomic control suggested that the genomic control *P* values that we reported were conservative.

The most highly associated SNPs in this study are located near the 5′ UTR of *GPCPD1*; a linkage disequilibrium block extends over the full length of the gene, and therefore, it is likely that the functional variant is located within this gene. This genetic proximity suggests a role for *GPCPD1* in the scaling of occipital cortex; the next closest protein-coding gene (*PROKR2*) is over 300 kb away, and previous GWASs have found functional genes near SNPs. For example, a GWAS of height in over 100,000 individuals identified 21 loci containing a known skeletal growth gene, and over one-half of those genes were closest to the associated SNP (41). However, we cannot exclude the possibility that the SNPs that we have found are associated with a more distal gene.

The DNA sequence of *GPCPD1* is highly conserved from mouse (89% identical) to fruit fly (48%), and the protein includes two conserved domains used in glycogen metabolism in mammals. This gene is widely expressed, including in adult mouse and human brains (35, 42), but its function has only been investigated in mouse skeletal muscle growth (43). Remarkably, in two human brains, only 11 genes genome-wide had significantly higher expression than *GPCPD1* in occipital cortex, including *MET*, *SCN1B*, and *GPR161*, which are involved in neurodevelopmental and neurophysiological processes (44–46). A common variant in the promoter of *MET* has been associated with twofold increased risk for autism spectrum disorder (47), and a mutation in *SCN1B* has been linked to generalized epilepsy (48). Altered expression of *GPCPD1* could possibly contribute to variation in cortical surface area through its role in energy metabolism. Primary visual cortex has two times the density of neurons as other cortical regions (4) and therefore, increased metabolic requirements. If genetic variation in *GPCPD1*

increased the metabolic efficiency of neurons or glia, then neurons could support larger axonal and dendritic arbors and thus, potentially, a larger visual cortex. Future work will need to establish the role of *GPCPD1* in human brain development, aging, and pathology.

In summary, we predict that rs238295 (or a closely linked functional variant) regulates expression of *GPCPD1* because of its close proximity to the 5′ UTR of this gene. The timing and location in the brain of this differential expression as well as the mechanism by which this gene influences visual cortical surface area remain to be elucidated. Understanding the role of genes that contribute to normal cortical architecture in humans is an important step to understanding the genetic mechanisms of visual perception and ultimately, cortical pathology in a host of heritable neuropsychiatric disorders.

Materials and Methods

TOP Subjects. Four hundred and twenty-one subjects from the TOP study were analyzed. These subjects included 181 controls, 94 subjects with schizophrenia spectrum disorder, 97 subjects with bipolar spectrum disorder, and 49 subjects diagnosed with major depressive disorder or psychotic disorder not otherwise specified; 48.7% of the subjects were women, and the subjects were aged 35 ± 10 y (range = 18–65 y).

Genotyping. DNA was genotyped on the Affymetrix 6.0 array as previously reported (52, 53), and 597,198 SNPs passed quality control filters (SNP call rate > 95%, minor allele frequency > 5%, Hardy–Weinberg disequilibrium $P < 1 \times 10^{-6}$) and were merged with HapMap 3 reference populations. All subjects self-reported Norwegian ancestry, and PCA of an allele-sharing distance matrix across all subjects did not suggest any non-European ancestry genetic outliers.

Brain imaging. MRI scans were performed with a 1.5 T Siemens Magnetom Sonata scanner equipped with a standard head coil. Acquisition parameters were optimized for increased gray/white matter image contrast. More details are in *SI Materials and Methods* and the work by Rimol et al. (51).

ADNI Subjects. Data used in the preparation of this article were obtained from the ADNI database (http://www.loni.ucla.edu/ADNI/); 482 subjects who self-reported as white and non-Hispanic included 180 controls and 302 individuals with MCI (39.2% women; aged 75.3 ± 6.6 y). We included ADNI subjects with MCI but not Alzheimer's disease from the replication sample in an attempt to balance the increased power that resulted from having a larger sample size with the increased noise caused by the pathological changes in cortical surface area that have been associated with these neurological disorders.

Genotyping. DNA was genotyped with the Illumina Human610-Quad BeadChip, and 514,073 SNPs passed quality control filters (SNP call rate > 95%, minor allele frequency > 5%, Hardy–Weinberg disequilibrium $P < 1 \times 10^{-6}$) and were merged with 34 European reference populations. PCA of an allele-sharing distance matrix was used to remove three individuals as non-European ancestry genetic outliers.

Imaging. MRI data were collected on 1.5-T scanners at many study centers across the United States. The Laboratory of Neuro Imaging (LONI) website (http://www.loni.ucla.edu/ADNI/Research/Cores/index.shtml) describes specific protocols. Raw digital imaging and communications in medicine MR images were downloaded from the ADNI data page of the public ADNI site at the LONI website (http://www.loni.ucla.edu/ADNI/Data/index.shtml) published in 2007.

PING Subjects. Data used in the preparation of this article were obtained from the PING database (http://ping.chd.ucsd.edu/); 278 subjects were included aged 14.2 ± 4.1 y (range = 6–21 y), and 47.8% of subjects were female.

Genotyping. DNA was genotyped with the Illumina Human660W-Quad BeadChip, and 494,082 SNPs passed quality control filters (sample call rate > 98%, SNP call rate > 95%, minor allele frequency > 5%, Hardy–Weinberg disequilibrium $P < 1 \times 10^{-6}$) and were merged with Hapmap European reference populations; 599 individuals were removed as genetic outliers based on PCA of an allele-sharing distance matrix. Additionally, 157 of the remaining subjects were removed, because they shared greater than 10% of alleles identical by descent with another subject.

Imaging. T1-weighted MRI data were collected on 3-T scanners at nine study centers across the United States. Specific MRI scanner protocols are available at the PING study website (http://ping.chd.ucsd.edu/).

Genotype Imputation. TOP, ADNI, and PING genotypes were independently merged with the HapMap CEU reference population, which also included genetic variant information from the sequencing by the 1,000 Genomes Project. MACH 1.0 was used to impute genotypes with the default settings, and only SNPs that passed imputation quality control ($R > 0.5$) were included for additional analysis.

Cortical Area Measurements. MRI scans were analyzed with software developed at the University of California at San Diego Multi-Modal Imaging Laboratory based on the freely available FreeSurfer software package (http://freesurfer-software.org/). Using cortical surface reconstruction and spherical atlas mapping procedures developed in the works by Dale et al. (52) and Fischl et al. (53), we mapped each individual's surface reconstruction into atlas space based on cortical folding patterns. Cortical folds are good predictors of the locations of functionally distinct regions (53). For example, there is close agreement between anatomical extent of primary visual cortex based on cortical folding patterns, functional MRI, and ex vivo cytoarchitecture (54).

Statistics. We tested each SNP for association using PLINK (55) to fit an additive linear model with minor allele count, sex, age, diagnosis, total cortical surface area, and a minor allele count by total cortical area interaction term as predictors of occipital cortical surface area. Genomic inflation (λ_{GC}) was estimated in the standard way by dividing the median observed χ^2 statistic from the GWAS by 0.456, the approximate median of a χ^2 distribution with one degree of freedom (56).

The permuted *P* value of the top SNP was calculated by shuffling subject labels ($n = 10^8$ permutations), recalculating the SNP interaction *P* values, and calculating the fraction of permutations that showed a more significant association than the *P* value derived from the original dataset. *P* values reported for the replication datasets are one-tailed, because we tested for an SNP effect in the same direction as in the original GWAS. In a meta-analysis of TOP, ADNI, and PING datasets, *P* values were combined based on inverse variance weighted *z* scores (34) calculated from the β-coefficients and genomic inflation-adjusted SEs (SE_{GC}). An association plot of combined *P* values was created using the SNAP plot online tool from the Broad Institute (57).

ACKNOWLEDGMENTS. We thank the study participants and the members of the Thematically Organized Psychosis Study group involved in data collection, especially Drs. Jimmy Jensen, Per Nakstad, and Andres Server. We also thank Eivind Bakken, Thomas Doug Bjella, Alan Koyama, Robin G. Jennings, Chris J. Pung, and Dr. Christine Fennema-Notestine. This work was supported by the Oslo University Hospital–Ullevål, South-Eastern Norway Health Authority Grant 2004-123, Research Council of Norway Grants 167153/V50 and 163070/V50, and Eli Lilly Inc. for parts of the genotyping costs of the TOP sample. Data collection and sharing for a portion of this project was funded by the Alzheimer's Disease Neuroimaging Initiative (ADNI; National Institute of Health Grant U01 AG024904). ADNI is funded by the National Institute on Aging and the National Institute of Biomedical Imaging and Bioengineering, and it is also funded through generous contributions from Pfizer Inc., Wyeth Research, Bristol-Myers Squibb, Eli Lilly and Company, GlaxoSmithKline, Merck and Co. Inc., AstraZeneca AB, Novartis Pharmaceuticals Corporation, Alzheimer's Association, Eisai Global Clinical Development, Elan Corporation plc, Forest Laboratories, and the Institute for the Study of Aging, with participation from the US Food and Drug Administration. Industry partnerships are coordinated through the Foundation for the National Institutes of Health. The grantee organization is the Northern California Institute for Research and Education, and the study is coordinated by the Alzheimer's Disease Cooperative Study at the University of California at San Diego. ADNI data are disseminated by the Laboratory of Neuroimaging at the University of California, Los Angeles. This work was also supported in part by National Institutes of Health Grants R01AG031224, R01AG22381, U54NS056883, P50NS22343, P50MH081755, 5UL1RR025774, U01DA024417, R01AG030474, R01MH080134, R01HL089655, U54CA143906, R01AG035020, R01DA030976, U19AG023122-01, R01MH078151-01A1, N01MH22005, and RC2DA029475. This work was also supported by the Price Foundation and Scripps Genomic Medicine.

1. Shyue SK, et al. (1995) Adaptive evolution of color vision genes in higher primates. *Science* 269:1265–1267.
2. Dominy NJ, Lucas PW (2001) Ecological importance of trichromatic vision to primates. *Nature* 410:363–366.
3. Halpern SD, Andrews TJ, Purves D (1999) Interindividual variation in human visual performance. *J Cogn Neurosci* 11:521–534.
4. Rockel AJ, Hiorns RW, Powell TP (1980) The basic uniformity in structure of the neocortex. *Brain* 103:221–244.

5. Duncan RO, Boynton GM (2003) Cortical magnification within human primary visual cortex correlates with acuity thresholds. *Neuron* 38:659–671.
6. Schwarzkopf DS, Song C, Rees G (2011) The surface area of human V1 predicts the subjective experience of object size. *Nat Neurosci* 14:28–30.
7. Andrews TJ, Halpern SD, Purves D (1997) Correlated size variations in human visual cortex, lateral geniculate nucleus, and optic tract. *J Neurosci* 17:2859–2868.
8. Dougherty RF, et al. (2003) Visual field representations and locations of visual areas V1/2/3 in human visual cortex. *J Vis* 3:586–598.
9. Chen CH, et al. (2011) Genetic influences on cortical regionalization in the human brain. *Neuron* 72:537–544.
10. Baaré WF, et al. (2001) Quantitative genetic modeling of variation in human brain morphology. *Cereb Cortex* 11:816–824.
11. Schmitt JE, et al. (2010) A twin study of intracerebral volumetric relationships. *Behav Genet* 40:114–124.
12. Wallace GL, et al. (2006) A pediatric twin study of brain morphometry. *J Child Psychol Psychiatry* 47:987–993.
13. Eyler LT, et al. (2011) Genetic and environmental contributions to regional cortical surface area in humans: A magnetic resonance imaging twin study. *Cereb Cortex* 21: 2313–2321.
14. Panizzon MS, et al. (2009) Distinct genetic influences on cortical surface area and cortical thickness. *Cereb Cortex* 19:2728–2735.
15. Tramo MJ, et al. (1998) Brain size, head size, and intelligence quotient in monozygotic twins. *Neurology* 50:1246–1252.
16. White T, Andreasen NC, Nopoulos P (2002) Brain volumes and surface morphology in monozygotic twins. *Cereb Cortex* 12:486–493.
17. Airey DC, Robbins AI, Enzinger KM, Wu F, Collins CE (2005) Variation in the cortical area map of C57BL/6J and DBA/2J inbred mice predicts strain identity. *BMC Neurosci*, 10.1186/1471-2202-6-18.
18. O'Leary DD, Chou SJ, Sahara S (2007) Area patterning of the mammalian cortex. *Neuron* 56:252–269.
19. Bishop KM, Goudreau G, O'Leary DD (2000) Regulation of area identity in the mammalian neocortex by Emx2 and Pax6. *Science* 288:344–349.
20. Leingärtner A, et al. (2007) Cortical area size dictates performance at modality-specific behaviors. *Proc Natl Acad Sci USA* 104:4153–4158.
21. Bayatti N, et al. (2008) Progressive loss of PAX6, TBR2, NEUROD and TBR1 mRNA gradients correlates with translocation of EMX2 to the cortical plate during human cortical development. *Eur J Neurosci* 28:1449–1456.
22. Sisodiya SM, et al. (2001) PAX6 haploinsufficiency causes cerebral malformation and olfactory dysfunction in humans. *Nat Genet* 28:214–216.
23. Mitchell TN, et al. (2003) Polymicrogyria and absence of pineal gland due to PAX6 mutation. *Ann Neurol* 53:658–663.
24. Brunelli S, et al. (1996) Germline mutations in the homeobox gene EMX2 in patients with severe schizencephaly. *Nat Genet* 12:94–96.
25. Faiella A, et al. (1997) A number of schizencephaly patients including 2 brothers are heterozygous for germline mutations in the homeobox gene EMX2. *Eur J Hum Genet* 5:186–190.
26. Merello E, et al. (2008) No major role for the EMX2 gene in schizencephaly. *Am J Med Genet A* 146A:1142–1150.
27. Tietjen I, et al. (2007) Comprehensive EMX2 genotyping of a large schizencephaly case series. *Am J Med Genet A* 143A:1313–1316.
28. Barak T, et al. (2011) Recessive LAMC3 mutations cause malformations of occipital cortical development. *Nat Genet* 43:590–594.
29. Rimol LM, et al. (2010) Sex-dependent association of common variants of microcephaly genes with brain structure. *Proc Natl Acad Sci USA* 107:384–388.
30. Joyner AH, et al. (2009) A common MECP2 haplotype associates with reduced cortical surface area in humans in two independent populations. *Proc Natl Acad Sci USA* 106: 15483–15488.
31. Price AL, et al. (2006) Principal components analysis corrects for stratification in genome-wide association studies. *Nat Genet* 38:904–909.
32. Courchesne E, et al. (2000) Normal brain development and aging: Quantitative analysis at in vivo MR imaging in healthy volunteers. *Radiology* 216:672–682.
33. Raznahan A, et al. (2011) How does your cortex grow? *J Neurosci* 31:7174–7177.
34. de Bakker PI, et al. (2008) Practical aspects of imputation-driven meta-analysis of genome-wide association studies. *Hum Mol Genet* 17:R122–R128.
35. Allen Human Brain Atlas (2011) *Allen Institute for Brain Science, Seattle, WA*. Available at http://human.brain-map.org. Accessed March 25, 2011.
36. Finlay BL, Darlington RB (1995) Linked regularities in the development and evolution of mammalian brains. *Science* 268:1578–1584.
37. Barton RA, Harvey PH (2000) Mosaic evolution of brain structure in mammals. *Nature* 405:1055–1058.
38. de Sousa AA, et al. (2010) Hominoid visual brain structure volumes and the position of the lunate sulcus. *J Hum Evol* 58:281–292.
39. Rakic P (1988) Specification of cerebral cortical areas. *Science* 241:170–176.
40. Chang EF, et al. (2010) Categorical speech representation in human superior temporal gyrus. *Nat Neurosci* 13:1428–1432.
41. Lango Allen H, et al. (2010) Hundreds of variants clustered in genomic loci and biological pathways affect human height. *Nature* 467:832–838.
42. Lein ES, et al. (2007) Genome-wide atlas of gene expression in the adult mouse brain. *Nature* 445:168–176.
43. Okazaki Y, et al. (2010) A novel glycerophosphodiester phosphodiesterase, GDE5, controls skeletal muscle development via a non-enzymatic mechanism. *J Biol Chem* 285:27652–27663.
44. Chen C, et al. (2004) Mice lacking sodium channel beta1 subunits display defects in neuronal excitability, sodium channel expression, and nodal architecture. *J Neurosci* 24:4030–4042.
45. Matteson PG, et al. (2008) The orphan G protein-coupled receptor, Gpr161, encodes the vacuolated lens locus and controls neurulation and lens development. *Proc Natl Acad Sci USA* 105:2088–2093.
46. Judson MC, Amaral DG, Levitt P (2011) Conserved subcortical and divergent cortical expression of proteins encoded by orthologs of the autism risk gene MET. *Cereb Cortex* 21:1613–1626.
47. Campbell DB, et al. (2006) A genetic variant that disrupts MET transcription is associated with autism. *Proc Natl Acad Sci USA* 103:16834–16839.
48. Wallace RH, et al. (1998) Febrile seizures and generalized epilepsy associated with a mutation in the Na+-channel beta1 subunit gene SCN1B. *Nat Genet* 19:366–370.
49. Athanasiu L, et al. (2010) Gene variants associated with schizophrenia in a Norwegian genome-wide study are replicated in a large European cohort. *J Psychiatr Res* 44: 748–753.
50. Djurovic S, et al. (2010) A genome-wide association study of bipolar disorder in Norwegian individuals, followed by replication in Icelandic sample. *J Affect Disord* 126:312–316.
51. Rimol LM, et al. (2010) Cortical thickness and subcortical volumes in schizophrenia and bipolar disorder. *Biol Psychiatry* 68:41–50.
52. Dale AM, Fischl B, Sereno MI (1999) Cortical surface-based analysis. I. Segmentation and surface reconstruction. *Neuroimage* 9:179–194.
53. Fischl B, Sereno MI, Tootell RB, Dale AM (1999) High-resolution intersubject averaging and a coordinate system for the cortical surface. *Hum Brain Mapp* 8:272–284.
54. Hinds O, et al. (2009) Locating the functional and anatomical boundaries of human primary visual cortex. *Neuroimage* 46:915–922.
55. Purcell S, et al. (2007) PLINK: A tool set for whole-genome association and population-based linkage analyses. *Am J Hum Genet* 81:559–575.
56. Devlin B, Roeder K, Wasserman L (2001) Genomic control, a new approach to genetic-based association studies. *Theor Popul Biol* 60:155–166.
57. Johnson AD, et al. (2008) SNAP: A web-based tool for identification and annotation of proxy SNPs using HapMap. *Bioinformatics* 24:2938–2939.